Subauroral morning proton spots (SAMPS) as a result of plasmapause-ring-current interaction

H. U. Frey,[1] G. Haerendel,[2] S. B. Mende,[1] W. T. Forrester,[3] T. J. Immel,[1] and N. Østgaard[1]

Received 30 March 2004; revised 28 May 2004; accepted 2 July 2004; published 15 October 2004.

[1] The proton aurora imager SI-12 on the IMAGE spacecraft occasionally observes subauroral morning proton spots (SAMPS) that rotate with 70–95% of the Earth's corotation speed. Coincident particle measurements by DMSP confirm the source to be pure precipitating protons with mean energies likely above the detector limit of 30 keV. The spots appear in the recovery phase after magnetic storms and last for 1–4 hours in the magnetic local time region of 0300–1200 hours. The latitude location is strongly related to the minimum Dst of the previous geomagnetic storm with the lowest latitude observations after the strongest storms. The rotation speed is related to the latitude (L shell) of the spots with the largest corotation lags for spots that map to the largest L shells. IMAGE-EUV observations of the plasmasphere indicate a relationship with density gradients in the expanding plasmasphere after magnetic storms. We interpret these spots as the result of wave-particle interaction. As one likely process, we suggest the interaction of ring current protons with electromagnetic ion-cyclotron (EMIC) waves as a result of the expansion and subrotation of the dense, cold plasmasphere ions. The appearance of subauroral proton spots is therefore a consequence of the plasmasphere refilling after geomagnetic storms. *INDEX TERMS:* 2704 Magnetospheric Physics: Auroral phenomena (2407); 2768 Magnetospheric Physics: Plasmasphere; 2788 Magnetospheric Physics: Storms and substorms; 2716 Magnetospheric Physics: Energetic particles, precipitating; 2483 Ionosphere: Wave/particle interactions; *KEYWORDS:* aurora, proton precipitation, wave-particle interaction, plasmapause, ring current

Citation: Frey, H. U., G. Haerendel, S. B. Mende, W. T. Forrester, T. J. Immel, and N. Østgaard (2004), Subauroral morning proton spots (SAMPS) as a result of plasmapause-ring-current interaction, *J. Geophys. Res.*, *109*, A10305, doi:10.1029/2004JA010516.

1. Introduction

[2] The aurora generally occurs in an oval between 60° and 75° magnetic latitude in both hemispheres. In addition, there are many other types of localized aurora at high latitude separated from the auroral oval. Most of these features like polar cap arcs [*Kullen et al.*, 2002], polar cap patches [*Walker et al.*, 1999], or high-latitude dayside aurora (HiLDA) [*Frey et al.*, 2004] occur during quiet geomagnetic conditions. FUV observations from the IMAGE spacecraft have also revealed several low-latitude auroras like the afternoon detached auroral arcs [*Immel et al.*, 2002; *Burch et al.*, 2002; *Spasojevic et al.*, 2004] and dayside detached arcs/proton flashes [*Zhang et al.*, 2002; *Hubert et al.*, 2003], the latter being a phenomenon of the arrival of a very strong disturbance in the solar wind.

[3] The plasmasphere is that magnetospheric region where the magnitude of the corotation electric field greatly exceeds the convection electric field and magnetic flux tubes are connected to the ionosphere for times of the order of days. The plasmapause, with its sharp gradient of cold plasma density and a decreasing magnetic field, is considered a significant source region of electromagnetic ion cyclotron wave (EMIC) generation [*Fraser and Nguyen*, 2001]. These waves occur predominantly in the afternoon (1400–1600 MLT) and at L values of 3–8 with the highest occurrence around L = 6–7. The waves can resonate with the local hot ion population of the adjacent ring current and were shown to cause afternoon subauroral arcs from pitch angle scattering of energetic ions [*Spasojevic et al.*, 2004].

[4] Here we report a new proton auroral feature. Occasionally, the IMAGE-FUV instrument observes subauroral morning proton spots (SAMPS). We will describe seven observations with their main properties, demonstrate their relation to plasmaspheric refilling after geomagnetic storms, and discuss interaction with EMIC waves as a possible cause. We will use observations made by the FUV [*Mende et al.*, 2000] and EUV [*Sandel et al.*, 2000] instruments on the IMAGE spacecraft.

2. Observations

[5] Figure 1 shows examples of SAMPS from 5 separate days, mapped to geomagnetic coordinates. SAMPS are very localized regions of enhanced Doppler-shifted Lyman-alpha emission well separated from the auroral oval at the low-

[1]Space Sciences Laboratory, University of California, Berkeley, California, USA.
[2]International University, Bremen, Germany.
[3]Lunar and Planetary Laboratory, University of Arizona, Tucson, Arizona, USA.

0148-0227/04/2004JA010516$09.00

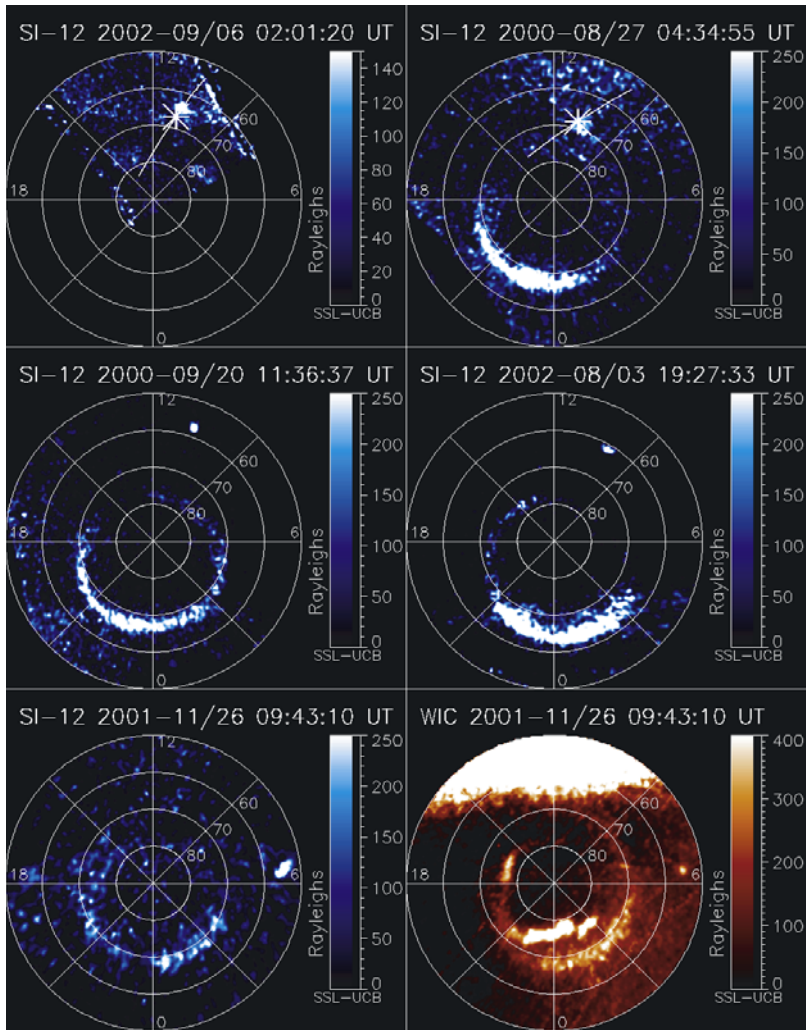

Figure 1. Examples of subauroral morning proton spots (SAMPS) observations on 5 different days. The bottom row shows proton and ''electron'' aurora images acquired simultaneously. The top images also show the DMSP ground tracks and the position at the time of image integration by the asterisks.

latitude morning sector. The size of these spots in the original proton aurora images is 2–3 pixels in each direction. As this is comparable to the size of the point spread function of the SI-12 imager, it is impossible to exactly determine the size of these spots. However, they appear to be less than 300 km in diameter. The spots are not very bright (less than 700 R) and are only visible due to the very low instrument background of the proton imager. Most of the time they appear suddenly within 2–3 images and change considerably in brightness. When they occur in the predawn region where the dayglow background is greatly reduced, they are also recognizable in the ''electron aurora'' images of FUV-WIC. This point will be further discussed later. All major properties of seven separate

Table 1. Major Properties of Subauroral Morning Proton Spots (SAMPS) Observations in IMAGE-FUV[a]

	2000–240 08–27	2000–264 09–20	2001–059 02–28	2001–209 07–28	2001–330 11–26	2002–215 08–03	2002–249 09–06
UT	0249–0528	1103–1223	0440–0725	1840–2020	0614–1028	1732–2120	0144–0221
Duration, h	2:39	1:20	2:45	1:40	4:14	3:48	0:37
Geog. Lat.	73.7	55.3	69.5	59.8	46.3	58.6	69.7
Geog. Lon.	90.8	329.7	29.9	253.4	290.6	235.4	134.5
Mag. Lat.	68.2°	56.9°	65.6°	68.3°	56.3°	63.0°	63.5°
L Shell	7.2	3.3	5.8	7.3	3.2	4.8	5.0
⟨MLT⟩	1030	1045	0840	1130	0430	1000	1050
Dst, nT	−5	−31	−4	4	−67	−12	−20
Min. Dst, nT	−24	−201	−37	−29	−221	−96	−104
Kp	1o	2+	1o	0+	2−	2o	2−
Corotation, %	78	92	72	78	88,85	88	95

[a]Locations are always given as the median values during the whole observation interval.

SAMPS observations are summarized in Table 1. Locations are always given as the median values during the whole observation periods.

[6] For two of the events we show the major solar wind and spot properties. On 27 August 2000 the SAMPS was observed for more than 2.5 hours and moved from 0900 to 1100 hours MLT (Figure 2). We used the MLT location to determine the corotation speed. The slope of the fitted line gives 78% of the corotation speed. The geomagnetic latitude did not change significantly over the observation period. The time-lagged IMF was northward and changed from positive to negative B_y just before the proton aurora imager was turned on and SAMPS was recognizable in the first images.

[7] On 26 November 2001 the first SAMPS was visible ~1 hour after the start of auroral observations (Figure 3). The IMF B_z changed from negative to positive and B_y changed from positive to negative during this observation. The motion of this spot occurred with 88% of the corotation speed until it disappeared below the visibility threshold of the proton aurora images. About half an hour later a new spot appeared at a slightly different location (1° latitude, 6° longitude) and rotated with 85% of the corotation speed.

[8] On 6 September 2002 the DMSP F15 spacecraft passed above the simultaneously observed SAMPS (see Figure 1, top left panel). The satellite first crossed a rather weak auroral oval between 77° and 69° magnetic latitude before encountering SAMPS at 63° magnetic latitude (0202) with a pure high-energy proton precipitation (Figure 4). It is impossible to determine the mean energy of the proton distribution because the proton fluxes are enhanced from 10 keV out to the detection threshold of the instrument at 30 keV. Therefore the protons have at least 20 keV mean energy but that is likely higher.

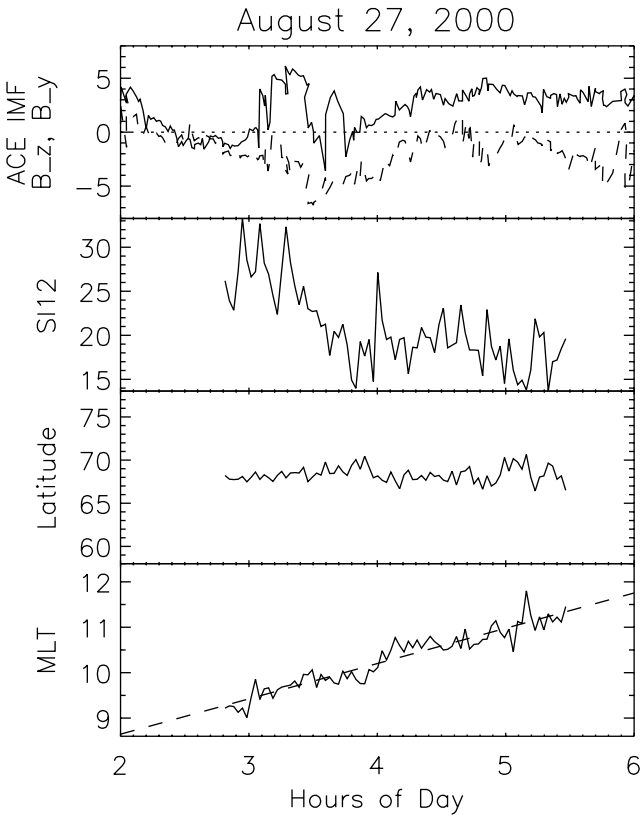

Figure 2. Summary of solar wind magnetic field and SAMPS properties on 27 August 2000. The top panel shows the time propagated ACE IMF measurements of B_z (solid line) and B_y (dashed line). The next panels show the maximum SI-12 instrument counts in the SAMPS and its geomagnetic latitude and local time. The bottom panel also shows the least squares fit to the MLT location that was used to determine the corotation speed as a dashed line.

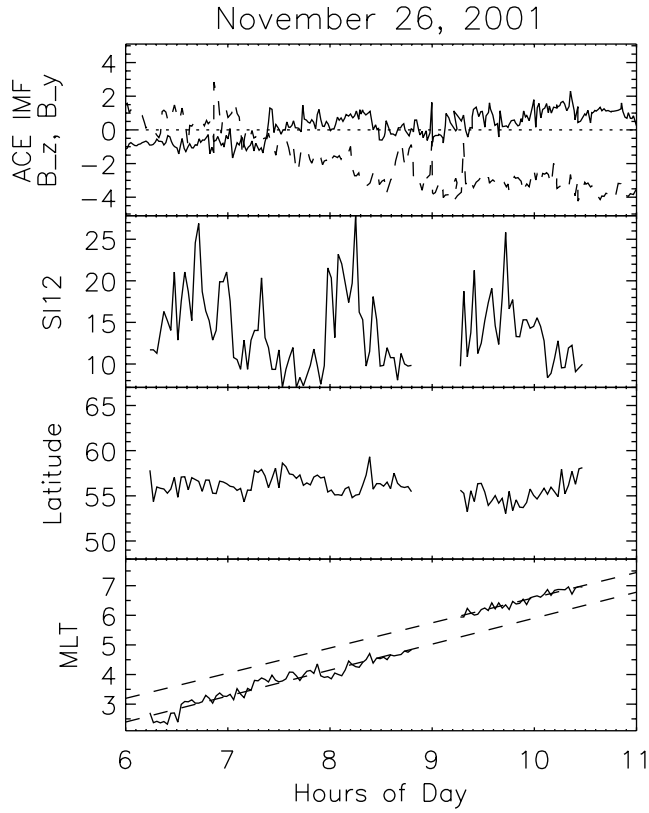

Figure 3. The same as Figure 3 for 26 November 2001.

[9] In another instance on 27 August 2000 the DMSP F14 spacecraft passed above the simultaneously observed SAMPS (see Figure 1, top right panel). The satellite first crossed a very weak auroral oval between 76° and 71° magnetic latitude before encountering SAMPS at 68° magnetic latitude (0435) with a weak low-energy and strong high-energy proton precipitation and a weak electron component at the high-latitude border of SAMPS (Figure 4). Again, there is a cutoff at the ion detector high-energy limit of 30 keV.

[10] Simultaneous images of the plasmasphere by IMAGE-EUV were obtained on 26 November 2001 and on 3 August 2002 and reveal a relationship between the SAMPS and structures of the plasmapause. Figure 5 shows examples how the SAMPS observed in five consecutive FUV frames (images every 2 min) map to the magnetic equatorial plane together with the EUV plasmasphere mapping (10 min integration). The dynamic range was exaggerated to clearly show the outer plasmasphere structures. The squares in the image represent the size of the spots when they are mapped from the ionosphere to the magnetic equator. On 26 November the EUV image shows a bulge [*Sandel et*

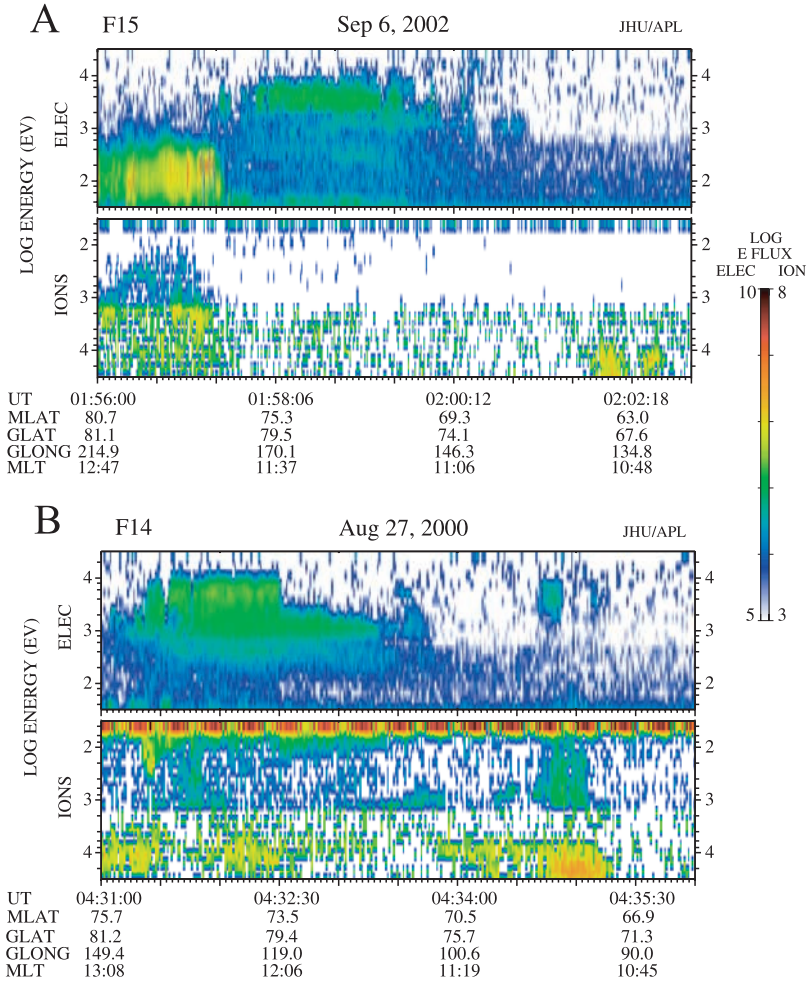

Figure 4. (a) Particle measurements by DMSP F15 on 6 September 2002 for precipitating electrons and ions. The satellite first crossed a rather weak auroral oval between 77° and 69° magnetic latitude before encountering SAMPS at 63° magnetic latitude with a pure high-energy proton precipitation. (b) The same as Figure 4a for DMSP F14 on 27 August 2000.

al., 2003] around 0500–0600 MLT and a notch at 0300–0400 MLT in the morning plasmapause. The SAMPS map into this notch with an approximate mapped size of 0.5 R_e. As the SAMPS corotated over time they later appeared to be related to a plasmapause notch at 1000 MLT (not shown). However, this notch coincided with the boundary between two of the EUV detectors and was not as obvious as in this 0806 UT example.

[11] On 3 August the EUV image shows a shoulder at 0900 local time. The shoulder extends out to about L = 4 and the SAMPS maps to the same location at larger distances of L = 4–5. Owing to the higher magnetic latitude when compared with the 26 November case, the mapped size of the spots is now ~1 R_e. Within these limits, the mapped locations basically overlap. An important question is if the precipitation is the result of a single localized source or a distribution of hot spots within the same region of plasmaspheric structures. However, for these two cases this question can not be answered with certainty.

[12] The SI-12 images were analyzed for the average rotational speed of the SAMPS (Figure 6). The average speed was 88% of corotation. Independently, the EUV images were analyzed to determine the average rotational speed of the shoulder with a result of 94% of corotation. This result is in agreement with previous reports of plasmaspheric rotational speeds and especially in good agreement with the SAMPS corotational speed. This fact supports the relationship between the appearance and motion of SAMPS and plasmaspheric structures.

[13] The 26 November 2001 event is not as clear because the gradient in the plasmaspheric notch is not very large. The notch structure appears and disappears in some EUV images and, as already mentioned above, later coincided with the boundary between two EUV detectors. Also, from FUV we know that the spot disappears and appears again at a slightly different location. A determination of the notch rotational speed was therefore impossible.

3. Discussion

[14] Observations of radial density structures (notches) of the plasmasphere have shown a rotation rate at L = 2–3 with an average lag to corotation of 10–15% [*Sandel et al.*, 2003] or 30% [*Adrian et al.*, 2004]. The ionospheric disturbance dynamo was identified as the cause of this lag [*Burch et al.*, 2004]. As the SAMPS observations show an

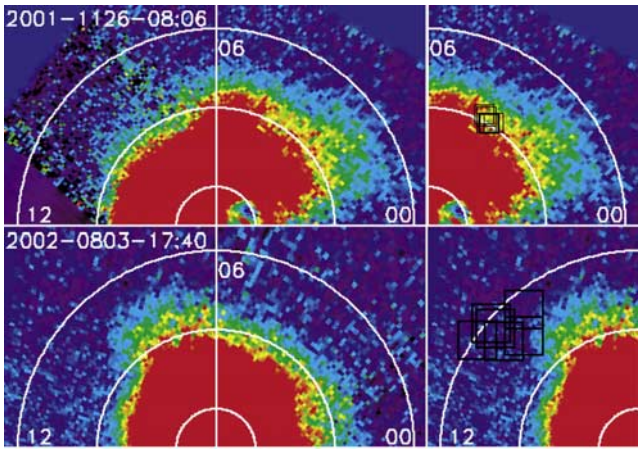

Figure 5. (top) EUV image of the plasmasphere at 0806 on 26 November 2001, as mapped to the geomagnetic equator. The dynamic range was exaggerated to show the notch in the plasmapause at L = 3 and MLT = 4 hours. The left part shows the EUV image with L = 3 and L = 5 rings and the noon meridian to the left. The right part shows the location of SAMPS at ±5 min around the EUV center time mapped to the magnetic equatorial plane. (bottom) The same for 3 August 2002 at 1740 UT when SAMPS were observed around 1000 MLT.

identical corotation lag of 10–30%, it is intriguing to assume a strong relationship between plasmaspheric density structures and SAMPS.

[15] Ions of gyrofrequency ω_c^+ can interact with ion cyclotron waves of frequency ω if $\omega < \omega_c^+$. The resonance energy E_R can be calculated as [*Kennel and Petschek*, 1966]:

$$E_R = E_{Mag}\left(\frac{\omega_c^+}{\omega}\right)^2\left(1-\frac{\omega}{\omega_c^+}\right)^3 \quad (1)$$

with the magnetic energy per particle

$$E_{Mag} = \frac{B^2}{2\mu_o n} = \frac{1}{2}mv_A^2. \quad (2)$$

Here n is the ion number density and v_A is the Alfvén speed of the ions. The SAMPS during our observations map to L = 3–7. If we perform a consistency check with an equatorial magnetic field of 500 nT at L = 4 and a density of 100 cm^{-3}, we obtain a magnetic energy per particle of 6.2 keV. The DMSP data indicate that the precipitating protons have mean energies above 30 keV, and in order to fulfill the resonance criterion, the frequency ratio in that case has to be $\frac{\omega}{\omega_c^+} \leq 0.28$. This is not an unreasonable value, especially as we do not know exactly the total ion density at the location of the resonance. With the above numbers we get a proton cyclotron frequency of $\omega_c^+ = 48$ s^{-1} and therefore a period of the resonating wave of 0.5 s. This period is in the range of Pc1 magnetic fluctuations and may be another evidence for a relation between optical auroral emissions and precipitation of energetic protons [*Mende et al.*, 1980].

[16] The mapping of SAMPS into the same region where the plasmapause shows an indentation (notch) or expansion (shoulder) gives rise to the assumption that they are caused by the expansion of the plasmasphere after the strong erosion during a geomagnetic storm [*Singh and Horwitz*, 1992; *Sandel et al.*, 2003], when there are still enhanced fluxes of trapped ring current ions. As the cold plasma of the plasmasphere corotates and interacts with the ring current, the lower-limit ion energy is lowered, allowing a larger fraction of the ring current ion distribution to locally interact with EMIC waves. The resonance then causes particle precipitation locally either at the density increase at the plasmapause or within single flux tubes of increased cold plasma density that may be too small to be resolved in EUV images but could explain the very localized appearance in the proton aurora images [*Carpenter et al.*, 2002]. Depending on their latitude position, the 300 km spots map to 3000–9000 km at the magnetic equator. However, this is rather an upper limit as the true spot size may be smaller (section 2).

[17] During the refilling of the plasmasphere, several wave-particle interactions were described [*Singh and Horwitz*, 1992]. They influence primarily the cold plasma that refills the emptied plasmasphere but may also interact with the hot ion population of the ring current [*Burch et al.*, 2001]. EMIC waves are just one possibility besides

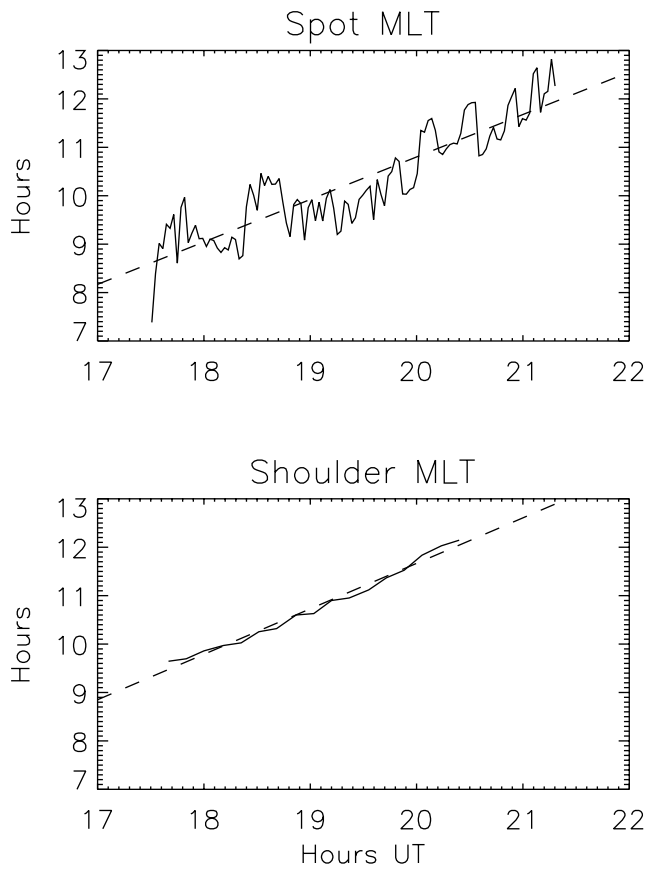

Figure 6. (top) Location of the proton spot on 3 August 2002 in magnetic local time. The least squares fitted average motion is 88% of corotation speed. (bottom) Location of the plasmaspheric shoulder that was observed simultaneously by IMAGE-EUV. The least squares fitted motion is 94% of the corotation speed.

electrostatic ion Bernstein waves and lower hybrid drift waves that can cause enhanced pitch angle scattering of ions [*Søraas et al.*, 1999]. The waves may be generated by the energetic ring current ions themselves or by electron beams, as may have been the case for the 27 August 2000 event (see Figure 4). More cases and especially simultaneous wave measurements by spacecraft like Polar or Cluster at the plasmapause should help to further investigate the likely cause of SAMPS.

[18] It is another question to be answered in further research if the SAMPS map into the low plasma density region of the notch in the 26 November case or if they map to the plasmapause at the notch, where there is the strong density gradient from the high-density plasmasphere to the lower-density outer region. The notch, that is the region of lower plasma density, is surrounded by higher plasma density. It is therefore harder to imagine how the lower plasma density could lower the EMIC instability threshold. One possibility could be that the early stage of cold plasma refilling may modify the instability criteria within the notch region. On the other hand it has to be noted that the dynamic range of Figure 5 was exaggerated to clearer show the mapping of SAMPS into the notch. A slightly different dynamic range would have moved the darker region of the image more outward, and the SAMPS would have mapped just inside of what appears to be the plasmapause. More examples have to be found and estimates of the plasma density conjugate to SAMPS could answer this question.

[19] The quantitative analysis of the proton and "electron" aurora images provides additional insight into the source of these spots. During the coincident DMSP particle measurements on 6 September, a precipitating flux of 0.15 mW/m^2 is measured (Figure 4). The quantitative calibration of SI-12 provides an expected signal of 17 counts per 1 mW/m^2 energy flux for protons of 25 keV mean energy [*Frey et al.*, 2003]. The measured 13 counts above background provide a 5 times brighter signal than expected, indicating that there are higher-energy protons missing in the DMSP measurements, as speculated in section 2. The coincident proton and "electron" aurora images at 0943 on 11 November 2001 show a WIC/SI-12 count ratio of 10 in the spot. For pure proton precipitation, that ratio is only expected for protons of 2 keV mean energy. We do not have coincident particle measurements for this case, but this low-energy value is in stark contrast to the DMSP observations on 6 September and 27 August. At higher proton energies the expected ratio is larger (20 for 8 keV protons), and this also excludes any additional electron precipitation contribution as this would rather increase the expected ratio for any proton energy and could never reduce the expected larger ratios down to the observed value of 10. We can only speculate that the true proton distribution was either not isotropic and kappa-like (as used for the model calculations in the work of *Gérard et al.* [2000] and *Frey et al.* [2003]), or made out of a bienergetic distribution, or of mean energy much higher than 50 keV. For proton energies above 100 keV it is expected that the WIC/SI-12 count ratio will again decline; however, such calculations have not been performed yet and have to be left for future work.

[20] Solar wind parameters from ACE and WIND were searched for obvious relationships to the occurrence of SAMPS (see Figures 2 and 3). There is some indication

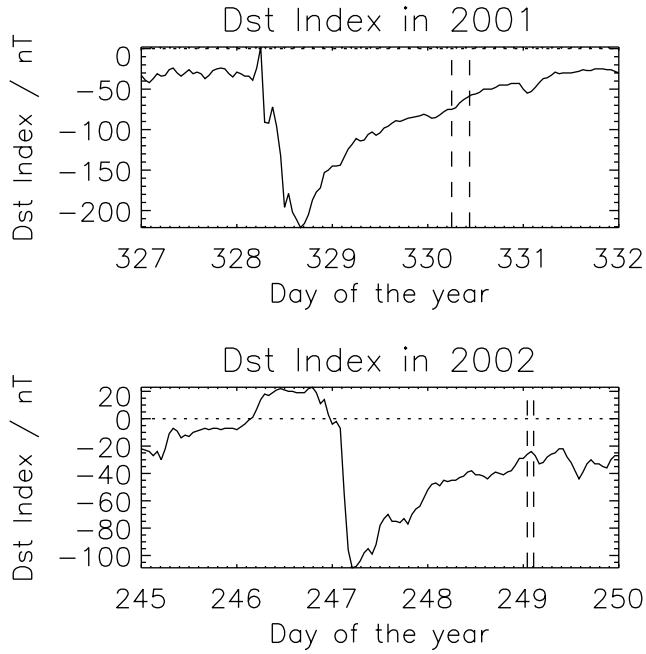

Figure 7. Geomagnetic Dst index around the periods of two SAMPS observations. Vertical lines mark the periods of SAMPS observations as shown in Table 1.

of a preferred occurrence during periods of low solar wind density and positive IMF B_z. However, the best relationship was found with geomagnetic indices Kp and Dst (Figure 7). All observed SAMPS occurred during the recovery period after a geomagnetic storm. Dst had generally recovered to about 1/5 of the minimum storm value and Kp was at or below 2.

[21] A very strong relationship was found between the geomagnetic latitude of SAMPS and the minimum Dst of the previous storm (Figure 8a). As the latitudes of the spots did not considerably change during the observation periods, the median values are good representations of their location. The lowest latitudes were found after the strongest storms and the correlation between both quantities is 0.98. Previous research with in situ measurements by the CRRES satellite showed that the plasmapause generally moved inward after storms on the nightside and dawnside [*Moldwin et al.*, 2003]. The observation of the strong relationship between the minimum Dst and the SAMPS latitude confirms this result with an even stronger correlation.

[22] Another relationship (though only R = −0.68) was found between the L shell of the SAMPS location and the corotation speed of the spot (Figure 8b). For spots at lower L shell (lower latitude), greater corotation speeds around 95% are found. For larger L shells (higher latitude) the corotation drops to ∼80%. This result is consistent with a strong corotational electric field at smaller geocentric distances, a reduced influence of it at larger distances, and the predictions of the ionospheric disturbance dynamo theory [*Burch et al.*, 2004].

[23] There is certainly a major morphological difference between the very localized SAMPS at the morningside and the elongated subauroral arcs in the afternoon. The event in the work of *Spasojevic et al.* [2004] demonstrated the

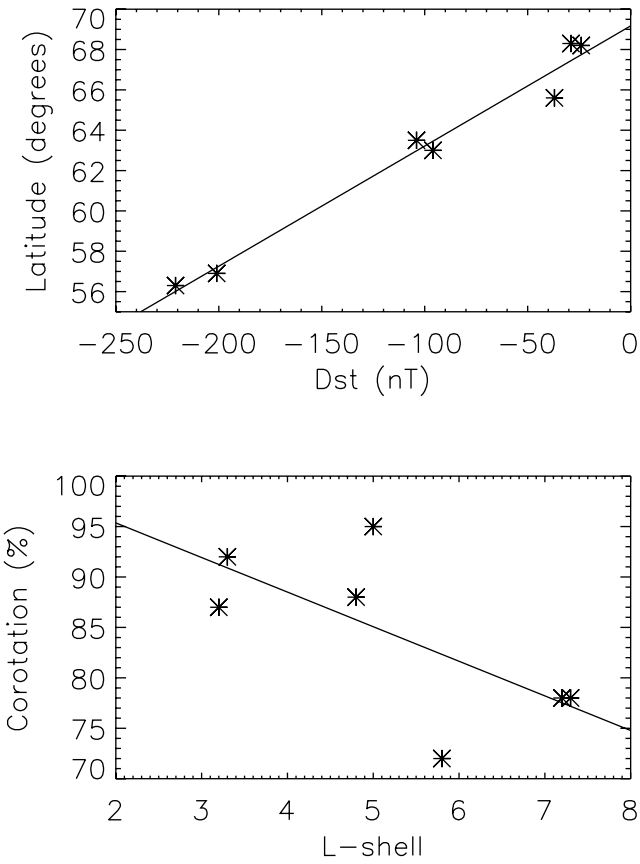

Figure 8. (top) Relationship between the latitude of SAMPS observation and the minimum Dst of the previous geomagnetic storm. The data are from Table 1 and the correlation is 0.98. (bottom) Relationship between the corotation speed of SAMPS and the L-shell of the location. The correlation coefficient is −0.68.

relationship between the extended plasmaspheric plume and the elongated subauroral arc. As that arc mapped to geosynchronous location, the coincident geosynchronous data supported the idea of a cause in EMIC waves. In our case we could only find the connection to the much smaller plasmaspheric notch and the shoulder extension which in part could explain the smaller size. Furthermore, satellite measurements demonstrated a much smaller probability of EMIC waves in the morning sector than in the afternoon [*Fraser and Nguyen*, 2001], and this could also explain that resonance regions are much more extended in the afternoon then in the morning.

4. Conclusions

[24] The observations in section 2 can be summarized as follows. Regions of very localized enhanced Doppler-shifted Lyman-alpha emission from protons of likely more than 30 keV energy occur in the morning sector between 0300 and 1200 MLT. They can last for 1–4 hours, are very stable in geomagnetic latitude, map to L shells of 3–7, and move with 70–95% of the corotation speed. They occur in the recovery phase after geomagnetic storms. Their geomagnetic latitude is determined by the minimum Dst of the preceding geomagnetic storm. Their corotational lag depends on the latitude (or L shell).

[25] The observations are not very frequent. The two major reasons are the occurrence after geomagnetic storms (which are not very frequent) and their low brightness that may prevent their detection after every storm. The strongest indication of a relationship to density structures in the plasmapause are their corotation with the same lag as plasmaspheric plumes [*Sandel et al.*, 2003; *Adrian et al.*, 2004], the very strong relationship between the latitude and the minimum Dst of the preceding storm, and their corotational lag according to their latitude. As the plasmapause is pushed inward during strong geomagnetic storms [*Sandel et al.*, 2003; *Moldwin et al.*, 2004], the slow plasmasphere expansion in the recovery phase must be one of the major conditions for the occurrence of SAMPS.

[26] It is not completely clear if the present observations describe the same phenomenon as the creation of stable auroral red (SAR) arcs from enhanced pitch angle scattering of protons [*Søraas et al.*, 1999]. SAR arcs are extended in local time, rather narrow in latitude, and were in the past described as resulting from electron precipitation [*Kozyra et al.*, 1982]. Our SAMPS are very localized in both local time and latitude and are caused by protons. More investigation is need to determine if these are two different phenomena or if a sensitivity issue prevents the SI-12 from observing the more extended arcs. Future work will also include investigation of a possible connection to magnetic pulsations on the ground [*Mende et al.*, 1980] and will extend the relationship to corotating plasmapause structures as seen by IMAGE-EUV. More investigation is also need to determine if EMIC wave interaction is really the dominating process or if electrostatic ion Bernstein waves, lower hybrid drift waves, or Coulomb scattering of ring current protons through the interaction with the cold plasmaspheric plasma account for the SAMPS creation.

[27] **Acknowledgments.** The authors acknowledge helpful discussion with George Parks and Michelle Thomsen. The DMSP particle detectors were designed by Dave Hardy of AFRL, and data were obtained from JHU/APL. We thank Dave Hardy, Fred Rich, and Patrick Newell for its use. The IMAGE FUV investigation was supported by NASA through SwRI subcontract 83820 at the University of California at Berkeley under contract NAS5-96020.

[28] Arthur Richmond thanks James Burch and Maria Spasojevic for their assistance in evaluating this paper.

References

Adrian, M. L., D. L. Gallagher, and L. A. Avanov (2004), IMAGE EUV observation of radially bifurcated plasmaspheric features: First observations of a possible standing ULF waveform in the inner magnetosphere, *J. Geophys. Res.*, *109*, A01203, doi:10.1029/2003JA009974.

Burch, J. L., D. G. Mitchell, B. R. Sandel, P. C. Brandt, and M. Wüest (2001), Global dynamics of the plasmasphere and ring current during magnetic storms, *Geophys. Res. Lett.*, *28*, 1159.

Burch, J. L., W. S. Lewis, T. J. Immel, P. C. Anderson, H. U. Frey, S. A. Fuselier, J.-C. Gérard, S. B. Mende, D. G. Mitchell, and M. F. Thomsen (2002), Interplanetary magnetic field control of afternoon-sector detached proton auroral arcs, *J. Geophys. Res.*, *107*(A9), 1251, doi:10.1029/2001JA007554.

Burch, J. L., J. Goldstein, and B. R. Sandel (2004), Cause of plasmasphere corotation lag, *Geophys. Res. Lett.*, *31*, L05802, doi:10.1029/2003GL019164.

Carpenter, D. L., M. A. Spasojevic, T. F. Bell, U. S. Inan, B. W. Reinisch, I. A. Galkin, R. F. Bemson, J. L. Green, S. F. Fung, and S. A. Boardsen (2002), Small-scale field-aligned plasmaspheric density structures inferred from the Radio Plasma Imager on IMAGE, *J. Geophys. Res.*, *107*(A9), 1258, doi:10.1029/2001JA009199.

Fraser, B. J., and T. S. Nguyen (2001), Is the plasmapause a preferred source region of electromagnetic ion cyclotron waves in the magnetosphere?, *J. Atmos. Sol. Terr. Phys.*, *63*, 1225–1247.

Frey, H. U., S. B. Mende, T. J. Immel, J.-C. Gérard, B. Hubert, S. Habraken, J. Spann, G. R. Gladstone, D. V. Bisikalo, and V. I. Shematovich (2003), Summary of quantitative interpretation of IMAGE far ultraviolet auroral data, *Space Sci. Rev.*, *109*, 255.

Frey, H. U., N. Østgaard, T. J. Immel, H. Korth, and S. B. Mende (2004), Seasonal dependence of localized, High Latitude Dayside Aurora (HiLDA), *J. Geophys. Res.*, *109*, A04303, doi:10.1029/2003JA010293.

Gérard, J.-C., B. Hubert, D. V. Bisikalo, and D. V. Shematovich (2000), A model of the Lyman-α line profile in the proton aurora, *J. Geophys. Res.*, *105*, 15,795.

Hubert, B., J.-C. Gérard, S. A. Fuselier, and S. B. Mende (2003), Observation of dayside subauroral proton flashes with the IMAGE-FUV imagers, *Geophys. Res. Lett.*, *30*(3), 1145, doi:10.1029/2002GL016464.

Immel, T. J., S. B. Mende, H. U. Frey, L. M. Peticolas, C. W. Carlson, J.-C. Gérard, B. Hubert, S. A. Fuselier, and J. L. Burch (2002), Precipitation of auroral protons in detached arcs, *Geophys. Res. Lett.*, *29*(11), 1519, doi:10.1029/2001GL013847.

Kennel, C. F., and H. E. Petschek (1966), Limit on stably trapped particle fluxes, *J. Geophys. Res.*, *71*, 1.

Kozyra, J. U., T. E. Cravens, A. F. Nagy, M. O. Chandler, L. H. Brace, N. C. Maynard, D. W. Slater, B. A. Emery, and S. D. Shawhan (1982), Characteristics of a stable auroral red arc event, *Geophys. Res. Lett.*, *9*, 973.

Kullen, A., M. Brittnacher, J. A. Cumnock, and L. G. Blomberg (2002), Solar wind dependence of the occurrence and motion of polar auroral arcs: A statistical study, *J. Geophys. Res.*, *107*(A11), 1362, doi:10.1029/2002JA009245.

Mende, S. B., R. L. Arnoldy, L. J. Cahill, J. H. Doolittle, W. C. Armstrong, and A. C. Fraser-Smith (1980), Correlation between λ4278-Å optical emissions and a Pc1 pearl event observed at Siple Station, Antarctica, *J. Geophys. Res.*, *85*, 1194.

Mende, S. B., et al. (2000), Far ultraviolet imaging from the IMAGE spacecraft, *Space Sci. Rev.*, *91*, 243–270.

Moldwin, M. B., S. Mayerberger, H. K. Rassoul, T. Barnicki, and R. R. Anderson (2003), Plasmapause response to geomagnetic storms: CRRES results, *J. Geophys. Res.*, *108*(A11), 1399, doi:10.1029/2003JA010187.

Moldwin, M. B., J. Howard, J. Sanny, J. D. Bocchicchio, H. K. Rassoul, and R. R. Anderson (2004), Plasmaspheric plumes: CRRES observations of enhanced density beyond the plasmapause, *J. Geophys. Res.*, *109*, A05202, doi:10.1029/2003JA010320.

Sandel, B. R., et al. (2000), The extreme ultraviolet imager investigation for the IMAGE mission, *Space Sci. Rev.*, *91*, 197–242.

Sandel, B. R., J. Goldstein, D. L. Gallagher, and M. Spasojevic (2003), Extreme ultraviolet imager observations of the structure and dynamics of the plasmasphere, *Space Sci. Rev.*, *109*, 25.

Singh, N., and J. L. Horwitz (1992), Plasmasphere refilling: Recent observations and modeling, *J. Geophys. Res.*, *97*, 1049.

Søraas, F., K. Aarsnes, J. A. Lundblad, and D. S. Evans (1999), Enhanced pitch angle scattering of protons at mid-latitudes during geomagnetic storms, *Phys. Chem. Earth*, *24*, 287.

Spasojevic, M., H. U. Frey, M. F. Thomsen, S. A. Fuselier, S. P. Gary, B. R. Sandel, and U. S. Inan (2004), The link between a detached subauroral proton arc and a plasmaspheric plume, *Geophys. Res. Lett.*, *30*, L04803, doi:10.1029/2003GL018389.

Walker, I. K., J. Moen, L. Kersley, and D. A. Lorentzen (1999), On the possible role of cusp/cleft precipitation in the formation of polar-cap patches, *Ann. Geophys.*, *17*, 1298–1305.

Zhang, Y., L. J. Paxton, T. J. Immel, H. U. Frey, and S. B. Mende (2002), Sudden solar wind dynamic pressure enhancements and dayside detached auroras: IMAGE and DMSP observations, *J. Geophys. Res.*, *107*(A12), 8001, doi:10.1029/2002JA009355.

W. T. Forrester, Lunar and Planetary Laboratory, University of Arizona, Tucson, AZ 85721, USA.

H. U. Frey, T. J. Immel, S. B. Mende, and N. Østgaard, Space Sciences Laboratory, University of California, Berkeley, CA 94720-7450, USA. (hfrey@ssl.berkeley.edu)

G. Haerendel, International University, Campus Ring 1, D-28759 Bremen, Germany.